AADE-16-FTCE-73

Field Study on Piezoresistive Smart Cement and Drilling Mud for Real Time Monitoring the Installation and Performance of the Cemented Well

C. Vipulanandan, K. Ali, B. Basirat, and A. Reddy, CIGMAT and THC-IT-University of Houston; D. Callahan, Layne.

Abstract

There are many issues related to cementing of the oil and gas wells onshore or offshore, well control operations are critical to ensure successful cementing of the oil wells without any losses. With increased drilling depths for production of oil and gas there are greater challenges due changes in the natural geological formations with in situ pressure and temperature conditions. Recent case studies on oil well failures have clearly identified cementing and drilling mud contamination as some of the issues that resulted in various types of delays in the cementing operations. For a successful cementing operation, it is critical to monitor the drilling and cementing operation during the installation so that necessary remediation can be made to minimize the delays and losses of cement. At present there is no technology available to monitor cementing operations without using buried sensors within the cement sheath and also monitor the movement of the drilling mud and spacer fluid to determine the changes real time during the installation of oil or gas wells.

In this study, a 40 feet long and 95/8 inch in diameter steel field well was installed and cemented using the smart cement mixture with enhanced piezoresistive properties. The field well was designed, built, and used to demonstrate the concept of real time monitoring of the flow of drilling mud and smart cement and hardening of the cement in place. The well was installed in soft swelling clay soils to investigate the sensitivity of the smart oil well cement. A new method has been developed to measure the electrical resistivity of the materials using the two probe method. Using the new concept, it has been proven that the resistivity dominated the behavior of drilling fluid and smart cement. LCR meters (measures the inductance (L), capacitance (C) and resistance (R)) were used at 300 kHz frequency to measure the changes in resistance. The 40 feet well instrumentation was outside the casing with 120 probes, 18 strain gages and 9 thermocouples. The strain gages and thermocouples were used to compare the sensitivity of these instruments to the two probe resistance measured in-situ in the cement. The electric probes used to measure the resistance were placed vertically at 15 levels and each level had eight horizontal probes. Change in the resistance of hardening cement is being continuously monitored since the installation of the field well. A method to predict the changes in electrical resistance of the hardening cement outside the casing (Electrical Resistance Model - ERM) with time has been developed. The ERM predicted the changes in the electrical resistances of the hardening cement outside the cemented casing very well. In addition, the pressure testing showed the piezoresistive response of the hardened smart cement and a piezoresistive model has been developed to predict the pressure in the casing from the change in resistivity in the smart cement.

Introduction

With some of the reported failures and growing interest in environmental and economic concerns in the oil and gas industry, integrity of the cement sheath is of major importance. Oil well cement serves many purposes in the cemented oil and gas wells. Foremost important among these is to form a sealing layer between the well casing and the geological formation referred to as the zone of isolation. Two studies done on blowouts on the U.S. outer continental shelf during the period of 1971 to 1991 and 1992 to 2006 clearly identified cementing failures as the major cause for blowouts (Izon et al. 2007). Cementing failures increased significantly during the second period of study when 18 of the 39 blowouts were due to cementing problems (Izon et al. 2007). Also the deep-water horizon blowout in 2010 in the Gulf of Mexico was due to cementing issues (Carter et al. 2014; Kyle et al. 2014). The explosion at the drilling rig, Deepwater Horizon, which explored oil and gas at the Macondo well claimed eleven lives and caused severe injuries and record-breaking sea pollution by the release of about five million barrels of crude oil (Cristou and Konstantinidou 2012). Therefore, proper monitoring and tracking the process of well cementing and the performance during the entire service life has become important to ensure cement integrity (Vipulanandan et al. 2014 (a)-(d)).

Electrical resistivity measurement has been used by many researchers to characterize the cement concrete and in other cement applications (McCarter 2000; Wei et al. 2008; Azhari et al. 2012; Liao et al. 2014; Vipulanandan et al. 2004, 2006, 2014 (a)-(d), 2015 (a)-(d)). Past studies have investigated the changes in electrical resistivity with applied stress referred to as piezoresistive behavior of modified cement-based and polymer composites (Vipulanandan et al. 2004, 2006). These studies showed that the changes in resistivity with the applied

stress were 30 to 50 times higher than the strain in the materials. Hence the change in resistivity has the potential to be used to determine the integrity of the materials. Past studies have reported that the interfacial factors are important in obtaining electrical resistivity from electrical resistance (Chung 2001). Limited studies have used electrical measurement methods to study the microstructural evolution in hydrating cement-based material systems (Wei et al. 2008; Zuo et al. 2014). Only recently electrical resistivity for characterizing oil well cements (Vipulanandan et al. 2014 (a)-(d), 2015 (a)-(d)).

The conventional methods of measuring the electrical resistivity of cementitious materials can be categorized into direct-current (DC) methods and alternating-current (AC) methods, both of which require electrodes for their measurements. Therefore, there is the potential for contact problems between the electrodes and the matrix, which could completely affect the accuracy of the measurement. Recent studies have suggested that replacing the DC measurement with the AC measurement can eliminate the polarization effect (Zhang et al. 2010 (a)-(b), Vipulanandan et al. 2013).

Smart Oil Well Cement

Cement slurry flowing ability and stability are the major requirements in well cementing. Oil and gas well cements (OWCs) are usually made from Portland Cement clinker or from blended hydraulic cements. OWCs are classified into grades based upon their Ca3AlnOp (Tricalcium Aluminate – C3A) content as ordinary (O), moderate sulphate resistant (MSR), and/or high sulphate resistant (HSR) types. Each class is applicable for a certain range of well depth, temperature, pressure, and sulphate environments. OWCs usually have lower C3A contents, are coarsely ground, and may contain friction-reducing additives and special retarders such as starch and/or sugars in addition to or in place of gypsum.

Cements such as Class G and Class H are considered to be two of the most used cements in OWC applications. These cements are produced by pulverizing clinker consisting essentially of calcium silicates (CanSimOp), with an addition of calcium sulphate (CaSO4) (John, 1992). Class H cement is produced by a similar process, except that the clinker and gypsum are ground relatively coarser than for a Class G cement, to provide a cement with a surface area generally in the range 220 - 300 m2/kg (John, 1992).

A smart cement has been developed (Vipulanandan et al. 2014a,b; Vipulanandan and Mohammed 2015a,b) which can sense any changes going on inside the borehole during cementing and during curing after the cementing job. The smart cement can sense the changes in the water cement ratio, different additives, and any pressure applied to the cement sheath in terms of piezoresistivity (Vipulanandan and Mohammed 2015a). The failure compressive strain for the smart cement was 0.2% at peak compressive stress (Vipulanandan et al. 2015b) and the resistivity change is of the order of several hundreds making it over 500 times more sensitive.

Objective

The major objective of this work was to demonstrate the monitoring of the installation of a field well and to verify the sensitivity of the piezoresistive smart cement to the changing surrounding conditions and the external stresses applied on it.

The specific objectives were as follows:

(1) Investigate the instrumentation outside the casing to monitor the changes in the electrical resistance during the installation and after cementing of the well.

(2) Measure and predict the changes in the electrical resistance of the hardening smart cement sheath outside the casing.

(3) Verify the sensitivity of the hardened Piezoresistive smart cement sheath.

Theory and Concept

Impedance Model (Vipulanandan et al., 2013)

Equivalent Circuit.

It is important to identify the most appropriate equivalent circuit to represent the electrical properties of a material to characterize its performace with time. In this study, different possible equivalent circuits were analyzed to find an appropriate equivalent circuit to represent smart cement and drilling fluid.

Case 1: General Bulk Material –Capacitance and Resistance

In the equivalent circuit for Case1, the contacts were connected in series, and both the contacts and the bulk material were represented using a capacitor and a resistor connected in parallel (Fig. 1).

In the equivalent circuit for Case 1, R_b and C_b are resistance and capacitance of the bulk material, respectively; and R_c and C_c are resistance and capacitance of the contacts, respectively. Both contacts are represented with the same resistance (R_c) and capacitance (C_c), as they are identical. Total impedance of the equivalent circuit for Case 1 (Z_1) can be represented as follows:

$$Z_1(\sigma) = \frac{R_b(\sigma)}{1+\omega^2 R_b^2 C_b^2} + \frac{2R_c(\sigma)}{1+\omega^2 R_c^2 C_c^2} - j\left\{\frac{2\omega R_c^2 C_c(\sigma)}{1+\omega^2 R_c^2 C_c^2} + \frac{\omega R_b^2 C_b(\sigma)}{1+\omega^2 R_b^2 C_b^2}\right\}, \quad (1)$$

where ω is the angular frequency of the applied signal. When the frequency of the applied signal is very low, $\omega \rightarrow 0$, $Z_1 = R_b + 2R_c$, and when it is very high, $\omega \rightarrow \infty$, $Z_1 = 0$.

Case 2: Special Bulk Material - Resistance Only

Case 2 is a special case of Case 1 in which the capacitance of the bulk material (C_b) is assumed to be negligible (Fig. 2). The total impedance of the equivalent circuit for Case 2 (Z_2) is as follows:

$$Z_2(\sigma) = R_b(\sigma) + \frac{2R_c(\sigma)}{1+\omega^2 R_c^2 C_c^2} - j\frac{2\omega R_c^2 C_c(\sigma)}{1+\omega^2 R_c^2 C_c^2}. \quad (2)$$

When the frequency of the applied signal is very low, $\omega \rightarrow 0$, $Z_2 = R_b + 2R_c$, and when it is very high, $\omega \rightarrow \infty$, $Z_2 = R_b$ (Fig. 3).

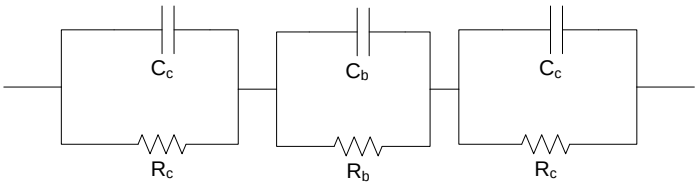

Figure 1. Equivalent Circuit for Case1

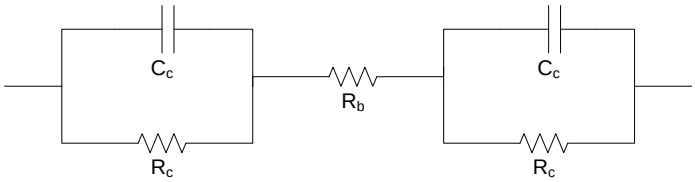

Figure 2. Equivalent Circuit for Case 2

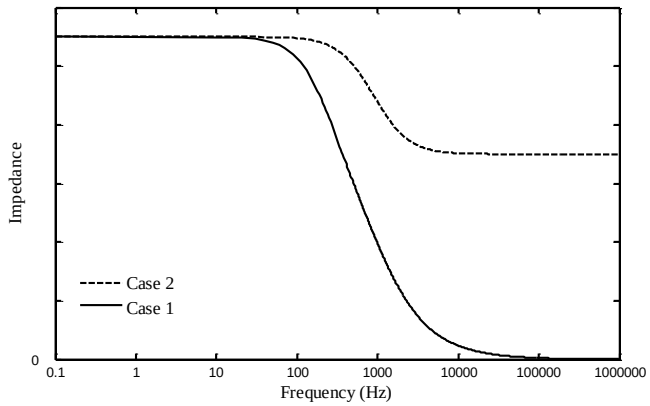

Figure 3. Comparison of Typical Responses of Equivalent Circuits for Case 1 and Case 2

The shape of the curves shown in Fig. 3 are very much influenced by the material response and the two probe instruments used for monitoring. Testing of smart cement and drilling fluid clearly indicated that Case 2 represented there behavior and hence the bulk material properties can be represeanted by resistivity and was characterized at a frequency of 300 kHz using the two probes in this study.

Resistance and Resistivity

After years of studies and based on the current study on well cements and drilling muds, electrical resistivity (ρ) was selected as the sensing property for both cements and drilling muds. This is unique since in that the same monitoring system can be used to evaluate the performance of cement and drilling muds. Hence, two parameters (resistivity and change in resistivity) will be used to quantify the sensing properties as follows:

$$R = \rho (L/A) = \rho K \quad (3)$$

where:

R = electrical resistance

L = Linear distance between the electrical resistance measuring points

A = effective cross sectional area

K = Calibration parameter is determined based on the resistance measurement method

Normalized change in resistivity with the changing conditions can be represented as follows:

$$\Delta\rho/\rho = \Delta R/R \quad (4)$$

Resistivity of the materials (ρ) to the changes (composition, curing, stress, fluid loss, and temperature) have been quantified. Correlating the changes, such as composition, curing, stress, cracking, fluid loss, and temperature, to the resistivity (ρ) (Eqn. (3)) and change in resistivity ($\Delta\rho$) (Eqn. (4)) will support the monitoring of the materials (cement and drilling fluid) behavior.

Test Site

After reviewing a few potential test sites, Energy Research Park (ERP) at the University of Houston, Houston Texas was selected to install the field well. Many factors including geology, swelling and soft clays, changing surrounding conditions (weather, active zone in the ground), environmental regulations and accessibility to the site for long-term monitoring had to be considered in selecting the test site since the focus of the study was to demonstrate the sensitivity of the smart cemented field well. The selected site had swelling clays with fluctuating moisture conditions (active zone) which represents the nearly the worst conditions that could be encountered when installing oil wells. The top 20 feet of the soil was swelling clay soil with liquid limit of over 50%. Based on ASTM classification, this soil was characterized as CH soil. The active zone in the Houston area is about 15 feet, indicating relatively large moisture fluctuation in the soil causing it to swell and shrink. The water table was 20 feet below gound and soil below the water table was also clay with less potential for swelling and the liquid limit was below 40%. Based on ASTM classification, this soil was characterized as CL soil.

Instrumentation

It has been shown that the two probes with AC current can be used to determine the electrical resistance changes in the smart cement and drilling fluid (Vipulanandan 2015 (a)-(d)). It was also important use other standard tools for measuring the changes in the cement sheath and compares it to the resistance changes. Because of practical reasons no instrument was placed on the casing and totally an independent system was developed to be place in the cement sheath. As shown in Fig. 4 and Fig. 5 probes were placed at various vertical depths. In the vertical direction the probes were placed at 15 levels (Fig. 4). Also eight probes (A, B, C, D, E, F, G and H) were

placed horizontally at each level. Also nine stain gages and nine thermocouples were included in the instrumentation (Fig. 4). When a vertical resistance measurement is referred as E 2-3, it refers to the measurement in column E between vertical levels 2 and 3. Similarly horizontal resistance measurement is referred as EF-2, measurement was done at vertical level 2 between probe E and probe F horizontally.

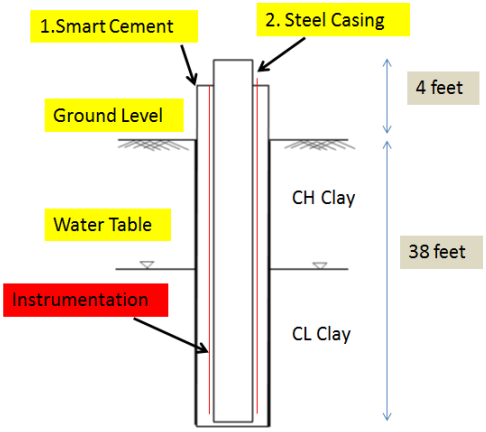

Figure 4. Schematic View of the Field Well with the Instrumentation

Installation of the Field Well

Layne Christensen Company, which is familiar with the drilling and cementing of wells in an urban setting, was selected to install the field well. A Texoma model 700 Pier Rig was used to drill the 16 in diameter bore hole and place the $9^{5}/_{8}$ in O.D. diameter carbon steel casing. The total length of the casing was 42 feet and needed pieces (including well head and needed connections to lift the casing) welded together to make a single unit. Initial twenty (20') feet was drilled without any drilling fluid. Polymer based drilling fluid was used to drill the balance of the borehole. After completing the drilling, the casing and the instrumentation units were centered and lowered into the borehole. Initial resistivity of vertical probes were measured (Fig. 6) in the air which was about 1000 Ω. The casing and the instrumentation were lowered into the borehole and the cement was pumped by use of a tremmie pipe, from the bottom of the borehole annulus to the surface, displacing the drilling mud. Monitoring of the resistance between the probes, temperature and stains (strain gages) were measured.

Materials and Methods

In this study, polymer drilling fluid and smart cement were used.

Polymer drilling fluid

Polymer based drilling fluids are used to drill through reactive geological formation. Since this study the drilling was to be done through swelling soft montmorillonite clay, polymer drilling fluid was used. It si less reactive with the clay formations and also controls the fluid loss into the formations. The density of the polymer drilling fluid was 8.7 ppg and the electrical resistivity was in the range of 2 Ω.m to 3 Ω.m.

Smart cement

Cement slurry was prepared using a water-to-cement ratio of about 0.6, making the mixing and pumping easier in the field. . The cement was modified with an addition of 0.075 percent conductive filler by total weight of the cement slurry. The initial resistivity of the cement slurry was in the range of 1.20 to 1.24 Ω.m. Total of 42 samples were collected for characterizing the smart cement behavior.

Initial resistivity of smart cement slurry

Two Different methods were used for electrical resistivity measurements of oil well cement slurries. To assure the repeatability of the measurements, the initial resistivity was measured at least three times for each cement slurry and the average resistivity was reported. The electrical resistivity of the cement slurries were measured using:

Conductivity probe

Commercially available conductivity probe was used to measure the conductivity (inverse of resistivity) of the slurries. In the case of cement, this meter was used during the initial curing of the cement. The conductivity measuring range was from 0.1μS/cm to 1000 mS/cm, representing a resistivity of 0.1Ω.m to 10,000 Ω.m.

Digital resistivity meter

Digital resistivity meter (used in the oil industry) was used measure the resistivity of fluids, slurries and semi-solids directly. The resistivity range for this device was 0.01 Ω -m to 400 Ω -m.

The conductivity probe and the digital electrical resistivity device were calibrated using standard solution of sodium chloride (NaCl).

Resistivity of smart cement

In this study high frequency AC measurement was adopted to overcome the interfacial problems and minimize the contact resistances. Electrical resistance (R) was measured using LCR meter during the curing time. This device has a least count of 1 μΩ for electrical resistance and measures the impendence (resistance, capacitance and inductance) in the frequency range of 20 Hz to 300 kHz. Based on the impedance (z) – frequency (f) response it was determined that the smart cement was a resistive material (Vipulanandan et al. 2013). Hence the resistance measured at 300 kHz using the two probe method was correlated to the resistivity (measured using the digital resistivity device) to determine the K factor (Eqn.1) for a time period of initial five hours of curing. This K factor was used to determine the resistivity of the cement with the curing time. The typical trend between impedance and frequency observed during the curing of smart cement is shown in Fig. 2.

Piezoresistivity test

Piezoresistivity describes the change in electrical resistivity of a material under stress. Since oil well cement serves as

pressure-bearing part of the oil and gas wells in real applications, the piezoresistivity of smart cement (stress – resistivity relationship) with different w/c ratios were investigated under compressive loading at different curing times. During the compression test, electrical resistance was measured in the direction of the applied stress. To eliminate the polarization effect, AC resistance measurements were made using a LCR meter at frequency of 300 kHz (Vipulanandan et al. 2013).

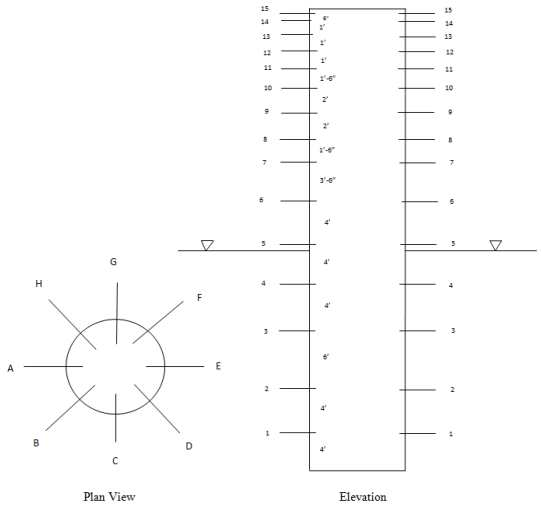

Figure 5 Vertical (Elevation) and Horizontal (Plan) Layout of the Probes in the Smart Cemented Well

Results and Discussion

Piezoresistive Relationship

Collected cement samples were cured under different conditions and the tested compressive loading after 45 days to determine the piezoresistivity. The bottom and middle level samples were cured under water and the top level sample was cured under room condition (23^{o}C and relative humidity of 50%). For a sample cured under water the change in the resistivity at peak stress varied was 74% and it varies based on the different batches of mixing of the smart cement. The compressive strength of the sample was 2595 psi. The failure compressive strain for the smart cement was 0.2% at peak compressive stress (Vipulanandan et al. 2015b) and hence the resistivity change was over 350 times more sensitive.

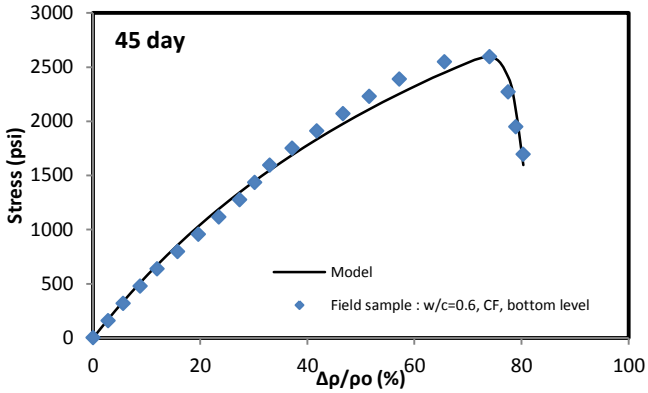

Figure 6 Piezoresistive Behavior of the Smart Cement At Various Depths in the Field Well

Based on experimental results, p-q model was modified to predict the change in electrical resistivity of cement during with applied compressive stress for 45 days of curing. The model is defined as follows:

$$\frac{\sigma}{\sigma_f} = \left[\frac{\frac{x}{x_f}}{q_2+(1-p_2-q_2)\frac{x}{x_f}+ p_2 \left(\frac{x}{xf}\right)^{\left(\frac{p_2+q_2}{p_2}\right)}} \right] \quad (5)$$

where σ is the stress (MPa); σ_f: compressive stress at failure (MPa); $x = \left(\frac{\Delta\rho}{\rho_o}\right) * 100$: Percentage of change in electrical resistivity due to the stress; $x_f = \left(\frac{\Delta\rho}{\rho_o}\right)_f * 100$: Percentage of change in electrical resistivity at failure; Δρ: change in electrical resistivity; ρ_o : Initial electrical resistivity (σ=0 MPa). The model parameter q_2 and p_2 were 0.55 and 0.011 respectively. The coefficient of determinations (R^2) was 0.98.

Installation

During initial 20 feet of drilling no drilling fluid was used. In order to stabilize the borehole polymer drilling fluid was used drill the rest of the hole. The total length of the borehole was about 38 feet. The steel casing with external instrumentation was lowered into the borehole and the changes in the resistance was started to be monitored. The vertical resistance between the adjucent probes were of the order of 1000 Ω as shown in Fig. 7. The resistance between probes A1-A2 reduced to about 200 Ω when probe 2 reached the drilling fluid. Similarly the resistance between other adjacent probes reduced when the probes were submerged into the drilling fluid. In 20 minutes the probe A10-A11 reduced to 200 Ω indicating the rate of lowering of the casing about 38 feet, This sudden changes in the resistance clearly showed the level of the casing that was lowered and submerged in the drilling fluid.

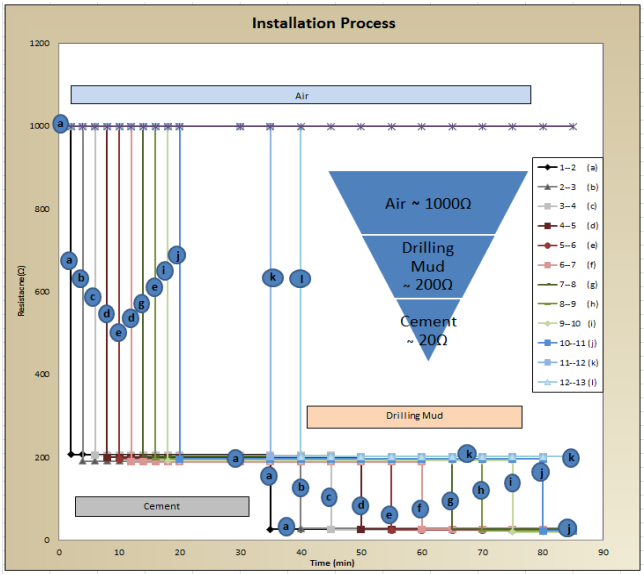

Figure 7 Vertical Resistance Changes for Drilling Fluid and Cement Slurry Reaching Various Levels

The cementing was started after 30 minutes. The resistance of probe A1-A2 (symbol **a** in Fig. 7) reduced to about 20 Ω after 35 minutes indicating that cement has reached vertical level 2. Rising of the cement lowered the resistances as shown in the Fig. 7. In about 80 minutes the cement reached the vertical level of 11 and the resistance dropped 20 Ω (A10-A11) (symbol **j** in Fig. 7). The electrical resistance changes observed during the placement of the drilling fluid and cement was very similar to the laboratory model test (Vipulanandan et al. 2015 (c)). Cement was displacing the drilling fluid at the top of the borehole and the vertical resistance (A12- A13) (symbol **l** in Fig. 7) dropped from 1000Ω to 200Ω indicating that drilling fluid has reached level 13 after 40 minutes of the operation.

Cement Curing

First Day

Typical changes measured in the strain gage, thermocouple and resistance probe during the first day of curing of the cement in the borehole are shown in Fig. 8. The thermocouple shows the increase in the temperature due to the hydration of the cement. The cement initial resistance was 24 Ω and reduced to about 20 Ω and then increased to about 50 Ω in 24 hours, a 150% change. The change in the strain gage resistance of 120 Ω was very small. Hence change in the electrical resistance was the largest of the parameter that are being monitored during the hydration of the cement..

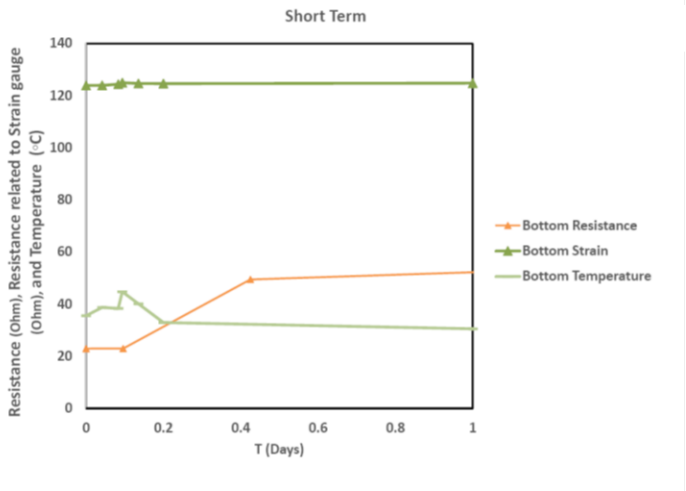

Figure 8 Variation in the Strain Gage, Temperature and Smart Cement Resistance During the First Day of Cement Curing in the Borehole.

Resistivity of the curing cement sheath with time

The resistivity of the cement slurry with curing time of up to 110 days was determined from the field samples in small molds (2 inches diameter and 4 inches height cylindrical mold) cured under different curing conditions. All field samples were first cured under room condition for one day then cured under no moisture loss condition (close to ground condition above the ground water), room condition and under water (representing the condition underwater. Samples cured under room condition had a weight loss of 2.8% after 110 days. The electrical resistivity was determined for a sample cured under moisture control (no moisture loss) condition, for a sample cured under room condition (a moisture loss of 2.8 % was calculated up to 110 days), and for a sample cured under water condition (a moisture gain of 1.2 % after 110 days) .

At least three specimens were tested under each condition and the average results are discussed. The change of electrical resistivity with curing time for the cement specimens cured under different environments is shown in Fig. 9. The normal trend of the resistivity of the cured cement is that the resistivity decreased up to a certain time (t_{min}) and reached to a minimum resistivity (ρ_{min}) and then starts increase with time. Hence the nonlinear model proposed by Vipulanandan and Paul (1990) was modified and used to predict the changes in the electrical resistivity of cement during hydration under different curing conditions and curing time. The proposed curing model is as follows:

$$\frac{1}{\rho} = \left(\frac{1}{\rho_{min}}\right)\left[\frac{\left(\frac{t+t_o}{t_{min}+t_o}\right)}{q_1+(1-p_1-q_1)*\left(\frac{t+t_o}{t_{min}+t_o}\right)+p_1*\left(\frac{t+t_o}{t_{min}+t_o}\right)^{\frac{q_1+p_1}{p_1}}}\right] \quad (6)$$

Where, ρ is the electrical resistivity (Ω-m); ρ_{min} is the minimum electrical resistivity (Ω-m); t_{min} is the time to reach the minimum electrical resistivity (ρ_{min}). The model

parameters were t_o, p_1 (t) and q_1 (t) and t was the curing time (min). The parameter q_1 represents the initial rate of change in the resistivity.

There are three characteristic resistivity parameters that can be used in monitoring the curing (hardening process) of the cement. The resistivity parameters are the initial resistivity (ρ_o), minimum electrical resistivity (ρ_{min}) and time to reach the minimum resistivity (t_{min}).

The resistivity shows an increasing trend with curing time (Fig. 9) which has been modeled with the curing model which is developed by modifying the p-q model proposed by Vipulanandan and Paul (1990) (Eqn. 6). The model parameters were for moisture control curing (zero weight loss): p_1=7.6, q_1=0.6, and t_o=70 min; for room curing: p_1=6.5, q_1=0.82, and t_o=72 min; and for under water curing: p_1=0.83, q_1=0.21, and t_o=58 min. (Table 1).

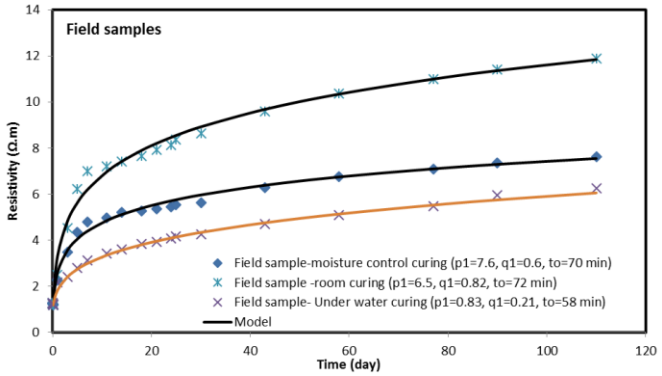

Figure 9 Variation of Smart Cement Resistivity with Curing Time for Samples Cured Under Room Condition (23°C and 50% Relative Humidity (RH)), Under Water and Zero Weight Loss.

The coefficient of determination (R^2) varied from 0.96 to 0.99 and the root mean square of error (RMSE) varied from 0.03 Ω.m to 0.72 Ω.m.

Table 1. Curing Model Parameters for Field samples

Curing Condition	Model Parameters				
	ρ_{min} (Ω.m)	t_{min} (min)	q	p	t_o (min)
Room curing	1.18	180	0.82	6.48	72
Moisture control curing	1.18	180	0.61	7.6	70
Under water curing	1.18	180	0.21	0.84	58

Prediction and Measured Resistance

The resistance measured on site can be predicted using Eqn. 3. Hence parameter K must be determined by calibrating the instrumentation.

Parameter K

The K parameter (i.e. L/A) for the wire setup A, B, C, D, E, F, G and H with the probe spacing were determined using the cement slurry. The resistivity of the cement slurry was measured by direct resistivity measurement device and the resistance between the two probes was measured using the LCR meter. The results of the K values are shown in Fig. 10 and the average value, maximum value, and minimum values are summarized in Table 3 for different wire combination.

For different wire combination, the average K parameter are found to be varied from 14.6 to 29.8 m^{-1} with standard deviations varying from 1.6 to 3.3 m^{-1} (Fig. 10).

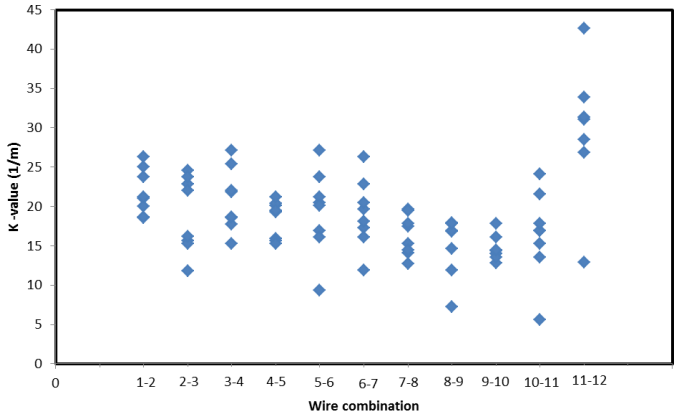

Figure10 Parameter K for Different Wire Combination for Instrumented Field Well

Predicted (Electrical Resistance Model –ERM)

Vertical Resistance

Probe F2-F3:. The measured vertical resistance between probes F2 and F3 (72 inches spacing) below the ground water are compared to the predicted resistance in Fig 11. With increased curing the measured resistance values were within

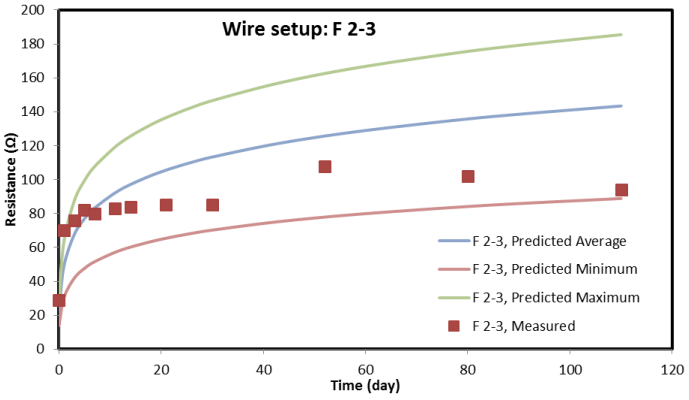

Figure 11 Comparing the Predicted and Measured Resistance for Vertical Probes F2-F3.

the predicted region. During the period of 110 days the electrical resistance changed from 24 Ω to 110 Ω, over 350%

increase in the resistance.

Probe F5-F6:. The measured vertical resistance between probes F5 and F6 (48 inches spacing) above the ground water are compared to the predicted resistance in Fig 12. The changes in the resistance are very similar to that was observed for probes F2-F3. The measured resistances during the period of 3 to 5 days were little higher than the predicted values. This may be because of the difference in the curing condition of the cement in the ground compared to the laboratory or small amount of clay soil contaminating the cement. . With increased curing the measured resistance values were within the predicted region. During the period of 110 days the electrical resistance changed from 20 Ω to 140 Ω, over 600% increase in the resistance.

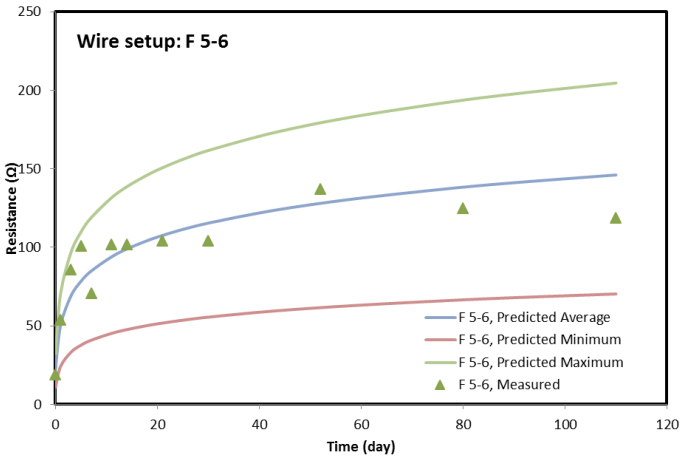

Figure 12 Comparing the Predicted and Measured Resistance for Vertical Probes F5-F6.

Horizontal Resistance

Probe E10-F10:. The measured horizontal resistance between probes E10 and F10 (5 inches spacing) close to the ground surface are compared to the predicted resistance in Fig 13. The changes in the resistance are very similar to that was observed for probes E2-E3 and E5-E6. With increased curing all the measured resistance values were within the predicted region. Unlike vertical Probe E10-E11, the measured resistances between probes E10 and F10 continuously increased and was not affected by the higher environmental temperature (hot weather during June-July in Houston) because the probes 2.5 feet below the ground surface. During the period of 110 days the electrical resistance changed from 18 Ω to 90 Ω, over 400% increase in the resistance.

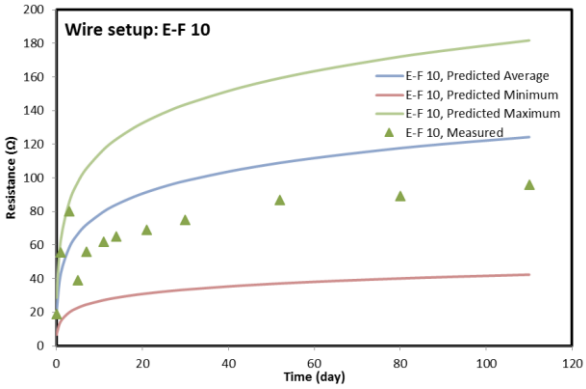

Figure 13 Comparing the Predicted and Measured Resistance for Horizontal Probes E2-E3.

Pressure Test

To simulate a pressure test, air pressure (P_i) was applied inside the tube (Fig. 14) to verify the piezoresistivity of the cement-sheath. Initially the electrical resistances (R_o in Ohms) were measured entire depth. These values were monitored while the air pressure was applied inside the casing (Figure 15) at a depth of 5 feet to a specific length of 18 inches using a expanding bladder. This test was done to demonstrate the sensitivity of the smart cement to the applied small pressures.

Case 1: Pi = 10 psi: Internal pressure of 10 psi was applied and the resistance changes were measured immediately. The change in resistance was normalized with initial resistance ΔR/R(%) is shown in Fig.14. The resistivity change in the smart cement due to the applied pressure was about 0.8 to 1.6 percent, indicating the piezoresistivity of the smart cement.

Case 2: Pi = 20 psi: Pressure of 20 psi was applied and the resistance changes were measured immediately and reported in the form of ΔR/R (%) in Fig. 14. The resistivity change in the smart cement due to the applied pressure of 20 psi was about 1.0 to 2.3 percent and was varying with the depth, indicating the piezoresistivity of the smart cement.

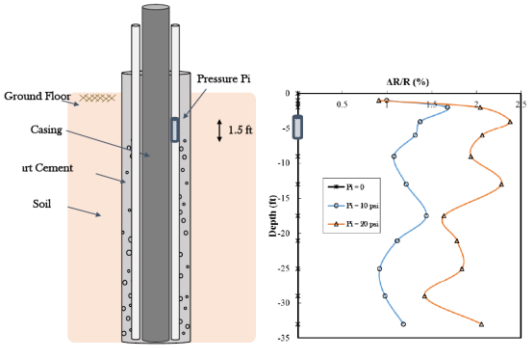

Figure 14 Variation of Initial Resistance with Depth after 100 Days of Curing

Piezoresistive modeling: The stress at every point can be separated into mean stress and deviatoric stress. The change in the deviatoric stress due to an applied pressure (Pi) along the axis of the casing (z-axis) is represented as ΔS_{zz}. Using equilibrium and stress analyses, it can be shown that ΔS_{zz} is directly proportional to the applied internal pressure, Pi (Eqn 5). Hence, the change in deviatoric stress can be represented as follows:

$$\Delta S_{zz} = f(Pi) \quad (7)$$

The variation of internal applied pressure with the resistivity of smart cement ($\Delta\rho_Z/\rho_Z$) is shown in Fig. 16, and the response of the smart cement is shown to be nonlinear.

p-q model (Vipulanandan et al. (1990))

The nonlinear p-q model was developed by Vipulanandan et al. (1990) and was used to predict $\Delta\rho_z/\rho_z$ variation with the applied pressure. The relationship can be represented as follows:

$$p_i\left(\frac{\Delta\rho}{\rho}\right) = \frac{\left(\frac{\Delta\rho}{\rho}\right)}{q + (1-p-q)\left(\frac{\Delta\rho}{\rho}\right) + p\left(\frac{\Delta\rho}{\rho}\right)^{\frac{p}{q-p}}} \quad (8)$$

The model parameters p and q were 0.89 and 0.28, respectively. Hence, it is possible to predict the pressure in the casing using Eqn. (8) and also the stress in the cement sheath using Eqn.(5) by measuring the change in resistivity of the smart cement.

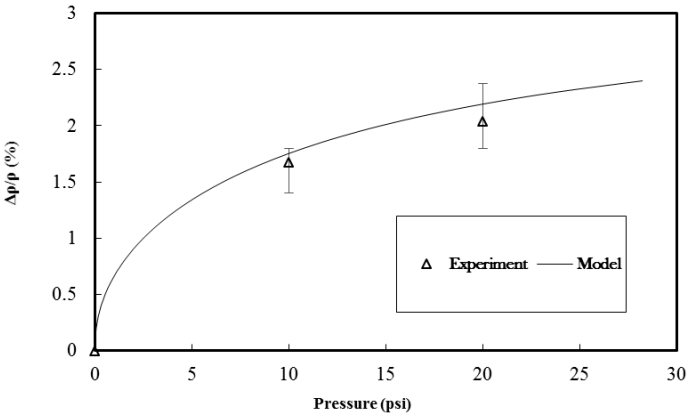

Figure 15 Model Predictions of Changes in Resistivity with Applied Pressure for Smart Cement after 100 Days of Curing

Conclusions

Based on the resistivity monitoring of the field installation, curing of the cement and piezoresistivity tests following conclusions are advanced:

(1) The two-probe method was effective in measuring the bulk resistance of the drilling fluid, and smart cement slurries. Based on the changes in resistance measurements it will be possible to identify the fluid rise in the well borehole.

(2) Field test demonstrate the potential of real-time monitoring of the levels of drilling fluid and smart cement slurries in the wellbore during installation.

(3) Based on the concept developed in this study, it was possible to predict the changes in the resistance of the hardening of smart cement. The predictions agreed well with the experimental results.

(4) The resistivity change in the smart cement used to cement the field well was very sensitive to the applied pressure, piezoresistive cement. Using a nonlinear p-q model the change in electrical resistivity of smart cement was related to the applied pressure in the casing.

(5) Constitutive models have been developed to represent the curing of the cement under various conditions. It is possible to predict the pressure in the casing and also the stress in the cement sheath using by measuring the change in resistivity of the smart cement.

Acknowledgements

This study was supported by the Center for Innovative Grouting Materials and Technology (CIGMAT) and the Texas Hurricane Center for Innovative Technology (THC-IT) at the University of Houston, Texas. Funding for the project (Project No. 10121-4501-01) is provided through the "Ultra-Deepwater and Unconventional Natural Gas and Other Petroleum Resources Research and Development Program" authorized by the Energy Policy Act of 2005. This program—funded from lease bonuses and royalties paid by industry to produce oil and gas on federal lands—is designed to assess and mitigate risk enhancing the environmental sustainability of oil and gas exploration and production activities. RPSEA is under contract with the U.S. Department of Energy's National Energy Technology Laboratory to administer three areas of research. RPSEA is a 501(c)(3) nonprofit consortium with more than 180 members, including 24 of the nation's premier research universities, five national laboratories, other major research institutions, large and small energy producers and energy consumers. The mission of RPSEA, headquartered in Sugar Land, Texas, is to provide a stewardship role in ensuring the focused research, development and deployment of safe and environmentally responsible technology that can effectively deliver hydrocarbons from domestic resources to the citizens of the United States. Additional information can be found at www.rpsea.org.

References

1. API Recommended Practice 10B (1997), Recommended Practice for Testing Well Cements Exploration and Production Department, 22nd Edition.
2. API Recommended Practice 65 (2002), Cementing Shallow Water Flow Zones in Deepwater Wells.

3. Carter, K. M. and Oort, E. (2014), Improved Regulatory Oversight Using Real- Time Data Monitoring Technologies in the Wake of Macondo, SPE 170323, pp. 1-51.
4. Chung, D.D.L. (2001). "Functional properties of cement-matrix composites." Journal of Material Science, Vol. 36, pp. 1315-1324.
5. Cristou, M., and Konstantinidou, M., (2012) "Safety of offshore oil and gas operations: Lessons from past accident analysis." Joint Research Centre of the European Commission, pp. 1-60.
6. Izon, D. and M. Mayes, M. (2007), "Absence of fatalities in blowouts encouraging in MMS study of OCS incidents 1992-2006," Well Control Magazine, pp. 86-90.
7. John B., (1992). "Class G and H Basic Oil Well Cements," World Cement.
8. Kyle, M. and Van Eric (2014), Improved regulatory oversight using real- time data monitoring technologies in the Wake of Macondo, SPE 170323, pp. 1-51.
9. Ramachandran, V. S. (1984), Concrete Admixture Handbook, Noyes Publication, Park Ridge, New Jersey, 628 pp.
10. Samsuri, A., Junin, R., and Osman, A.M. (2001), The utilization of Malaysian local bentonite as an extender and free water controller in oil-well cement technology, Society of Petroleum Engineers. Doi: 10.2118/68674-MS.
11. Sarap, G.D., Sivanandan, M., Patil, S., and Deshpande, A.P. (2009), The use of high performance spacers for zonal isolation in high temperature High-pressure wells SPE/IADC 124275.
12. Thaemlitz, J., A. D. Patel, et al. (1999). "New environmentally safe high-temperature water-based drilling-fluid system." SPE Drilling & Completion Vol. 14(3), 185-189.
13. Vipulanandan, C. and Paul, E. (1990) "Performance of epoxy and polyester polymer concrete," ACI Materials Journal, Vol. 87, No. 3, pp. 241–251.
14. Vipulanandan, C., and Sett, K. (2004), "Development and Characterization of Piezoresistive Smart Structural Materials", Proceedings, Engineering, Construction and Operations in Challenging Environments, Earth & Space 2004, ASCE Aerospace Division, League City, TX, pp. 656-663.
15. Vipulanandan, C., and Liu, J. (2005), "Polyurethane Based Grouts for Deep Off-Shore Pipe-in-Pipe Application", Proceedings, Pipelines 2005, ASCE, Houston, TX, pp. 216-227.
16. Vipulanandan, C., and Garas, V. (2006), "Piezoresistivity of Carbon Fiber Reinforced Cement Mortar", Proceedings, Engineering, Construction and Operations in Challenging Environments, Earth & Space 2006, Proceedings ASCE Aerospace Division, League City, TX, CD-ROM.
17. Vipulanandan, C., Dimrican, E., and Harendra, S. (2010), "Artificial Neural Network and Nonlinear Models for Gelling and Maximum Curing Temperature Rise in Polymer Grouts," Journal of Materials in Civil Engineering, Volume 23, No. 4, p. 1-6.
18. Vipulanandan, C. and Prasanth, P., (2013)" Impedance Spectroscopy Characterization of a piezoresistive Structural Polymer Composite Bulk Sensor," Journal of Testing and Evaluation, Vol. 41, No.6, 898-904.
19. Vipulanandan et al. (2014a), "Development and Characterization of Smart Cement for Real Time Monitoring of Ultra-Deepwater Oil Well Cementing Applications, OTC-25099-MS.
20. Vipulanandan et al. (2014b), "Characterization of Smart Cement Modified with Sodium Meta Silicate for Ultra-Deepwater Oil Well Cementing Applications, AADE-2014.
21. Vipulanandan, C. Heidari, M., Qu, Q., Farzam, H., and Pappas, J. M. (2014c), "Behaviour of piezoresistive smart cement contaminated with oil based drilling mud," Offshore Technology Conference, OTC 25200-MS, pp. 1-14.
22. Vipulanandan, C. and Mohammed, A. (2014d), "Hyperbolic rheological model with shear stress limit for acrylamide polymer modified bentonite drilling muds," Journal of Petroleum Science and Engineering, 122 (2014), 38–47.
23. Vipulanandan, C., and Mohammed, A., (2015a) "Smart cement rheological and piezoresistive behavior for oil well applications." Journal of Petroleum Science and Engineering, V-135, 2015, pp. 50-58.
24. Vipulanandan, C., and Mohammed, A., (2015b) "Smart cement modified with iron oxide nanoparticles to enhance the piezoresistive behavior and compressive strength for oil well applications." Journal of Smart Materials and Structures, Vol. 24 Number 12, pp. 1-11.
25. Vipulanandan, C, Krishnamoorti, R. Mohammed, A., G. Narvaez, Head, B. and Pappas, J. (2015c) "Iron Nanoparticle Modified Smart Cement for Real Time Monitoring of Ultra Deepwater Oil Well Cementing Applications", Offshore Technology Conference (OTC) 2015, OTC-25842-MS, pp. 1-20..
26. Vipulanandan, C, Ramanathan, P. Ali, M., Basirat, B. and Pappas, J. (2015d) "Real Time Monitoring of Oil Based Mud, Spacer Fluid and Piezoresistive Smart Cement to Verify the Oil Well Drilling and Cementing Operation Using Model Tests", Offshore Technology Conference (OTC) 2015, OTC-25851-MS, pp. 1-18.
27. Wei, X., Lianzhen, X. and Li, Z. (2008). "Electrical measurement to assess hydration process and the porosity formation." Journal of Wuhan University of Technology-Material Science. Ed., Vol. 23, pp. 761-766.
28. Zhang, M., Sisomphon, K., Ng, T.S, and Sun, D.J, (2010a). "Effect of superplasticizers on workability retention and initial setting time of cement pastes," Construction and Building Materials 24, 1700–1707.
29. Zhang, J., Weissinger, E.A, Peethamparan, S, and Scherer, G.W., (2010b). "Early hydration and setting of oil well cement," Cement and Concrete research, Vol. 40, 1023-1033.\
30. Zuo, Y., Zi, J. and Wei, X. (2014). "Hydration of cement with retarder characterized via electrical resistivity measurements and computer simulation." Journal of Construction and Building Materials